

3D Inversion of Large Scale Marine Controlled-Source Electromagnetics

Eldad Haber

*University of British Columbia
Vancouver, BC, Canada
eldadhaber@gmail.com*

Mike McMillan

*Computational Geosciences
Vancouver, BC, Canada
mike@compgeoinc.com*

Ben Kary*

*Computational Geosciences
Vancouver, BC, Canada
ben@compgeoinc.com*

Dave Marchant

*Computational Geosciences
Vancouver, BC, Canada
dave@compgeoinc.com*

SUMMARY

Three-dimensional controlled-source electromagnetic (CSEM) surveys can be a useful technique for oil and gas hydrate detection in marine environments. Electromagnetic waves are emitted from sources, and the ensuing electric and/or magnetic fields are recorded at one, or more receivers. The number, frequency, and position of sources and the placement of receivers depends on the particular application. The solution of an inverse problem is required to recover the earth's conductivity, which can be either isotropic or anisotropic in nature.

A major issue with either an isotropic or anisotropic CSEM inversion is the computational cost associated with the solution of many linear systems of equations. This is a result of a large spatial domain potentially containing complicated bathymetry, as well as the existence of thousands of source and frequency combinations. Overall, there could be thousands or even millions of systems of equations to solve on expansive meshes. To assist with these numerical issues, we use ideas developed for airborne electromagnetic inversions. First, we incorporate a locally refined mesh for the forward problem, specifically optimized for a source and set of receivers. Second, we use stochastic programming techniques to solve the CSEM problem with many sources and receivers. These methods dramatically reduce the numerical cost of each forward model as well as the total number of simulations. In this work we describe the methods used to overcome these computational difficulties.

Key words: Inversion, Electromagnetics, Marine

INTRODUCTION

3D controlled-source electromagnetic (CSEM) inversion can be a useful technique for oil and gas hydrate detection in marine environments. Electromagnetic waves are emitted from sources at a particular frequency, and ensuing electric and/or magnetic field information is recorded by a collection of receivers. The number, frequency and positions of sources and the placement of receivers depends on the characteristics of the respective application. To recover the earth's conductivity, an inverse problem is solved; producing a conductivity model that can reproduce the observed data. When a-priori information suggests that anisotropy is present, the conductivity is no longer scalar, and this can cause erroneous models to occur if an isotropic conductivity is assumed.

CSEM imaging techniques are now common, but solving for anisotropic conductivity in 3D is still relatively new (Newman et al., 2010). Generally, the CSEM inverse problem is set up as a discrete optimization problem where the residual between observed and predicted data is minimized with some form of regularization subject to constraints. Forward modelling of electromagnetic fields requires the numerical solution of Maxwell's equations. For a given mesh, this is achieved through finite difference, finite volume or finite element approaches (Schwarzbach et al., 2011).

A major issue with either an isotropic or anisotropic CSEM inversion is the computational cost associated with the solution of many linear systems of equations. This is a result of a large spatial domain potentially containing complicated bathymetry, as well as the existence of thousands of source locations and frequency combinations. Overall, there could be thousands or even millions of systems of equations to solve for on expansive meshes. To assist with these numerical issues, we use two ideas developed in Haber and Schwarzbach (2014) for airborne electromagnetic inversion. First, we incorporate a locally refined mesh for the forward problem, specifically optimized for a source and set of receivers. Second, we use stochastic programming techniques, in particular, proximal SAA methods (Ruszczynski and Shapiro, 2003) to solve the CSEM problem with many sources and receivers. These methods dramatically reduce the numerical cost of each forward model as well as the total number of simulations that are required to run the inversion.

For the anisotropic inversion, we separate the problem into two steps. First, we solve for a horizontal conductivity, then we fix this conductivity and solve for scale factors that relate the horizontal and vertical conductivities.

METHOD

Electromagnetic problems are governed by Maxwell's Equations. Maxwell's Equations with an isotropic conductivity are

$$\begin{aligned}\nabla \times \vec{E}_{jk} + i\omega\vec{B}_{jk} &= 0 \\ \nabla \times \mu^{-1}\vec{B}_{jk} - \Sigma\vec{E}_{jk} &= \vec{q}_k \\ \vec{n} \times \vec{B} &= 0\end{aligned}$$

Here, \vec{E} is the electric field, \vec{B} is the magnetic flux density, \vec{q} contains the external current density sources, μ is the magnetic permeability, ω is the angular frequency, Σ is the tensor conductivity, j is the frequency index, k is the transmitter index and \vec{n} is a normal vector. Typically, in field experiments we have a small number of frequencies, n_f but many more (thousands) of sources, n_s . Here we choose boundary conditions on the tangential components of \vec{B} but we can implement other boundary conditions as well that are equally appropriate.

Three primary difficulties are encountered when discretizing the system. First, the conductivity Σ varies over several orders of magnitude. Second, the curl operator possesses a non-trivial null-space, and the resulting linear systems are highly ill-conditioned. This negatively affects the performance of iterative solvers and direct methods are thus a preferable option if the problem size is sufficiently small. Third, the fields may change rapidly close to the sources while becoming smooth some distance away from the sources. This requires a sufficiently fine mesh around each source, but allows coarsening far from the source. To alleviate these problems, we use a locally refined OcTree mesh (see Schwarzbach et al. (2011) for OcTree meshes used with Maxwell's equation).

For problems with a few sources and receivers, or when the sources and receivers are in the same area, it is possible to use a single mesh for all sources, receivers and model features. Discretizing Maxwell's equation on this mesh leads to a single linear system to be solved for all sources and receivers. However, for problems where the domain of interest is large, this methodology is not feasible. If we were to perform all the computations on a single mesh, that mesh would have to contain hundreds of millions of degrees of freedom and the problem would be intractable. One way to bypass this difficulty is by using two steps. In the first, the forward modelling mesh is decoupled from the inversion mesh. In the second step, individual meshes are built for each source/receiver position. While this leads to tens of thousands of meshes for the solution of the forward model, each mesh is rather small and therefore, the forward problem on this mesh can be quickly carried out. Furthermore, since each forward problem can be carried out individually, this step is easily parallelized and is optimally scalable (if the number of nodes used for the computation is smaller than the number of sources). This concept is demonstrated in the Figure 1.

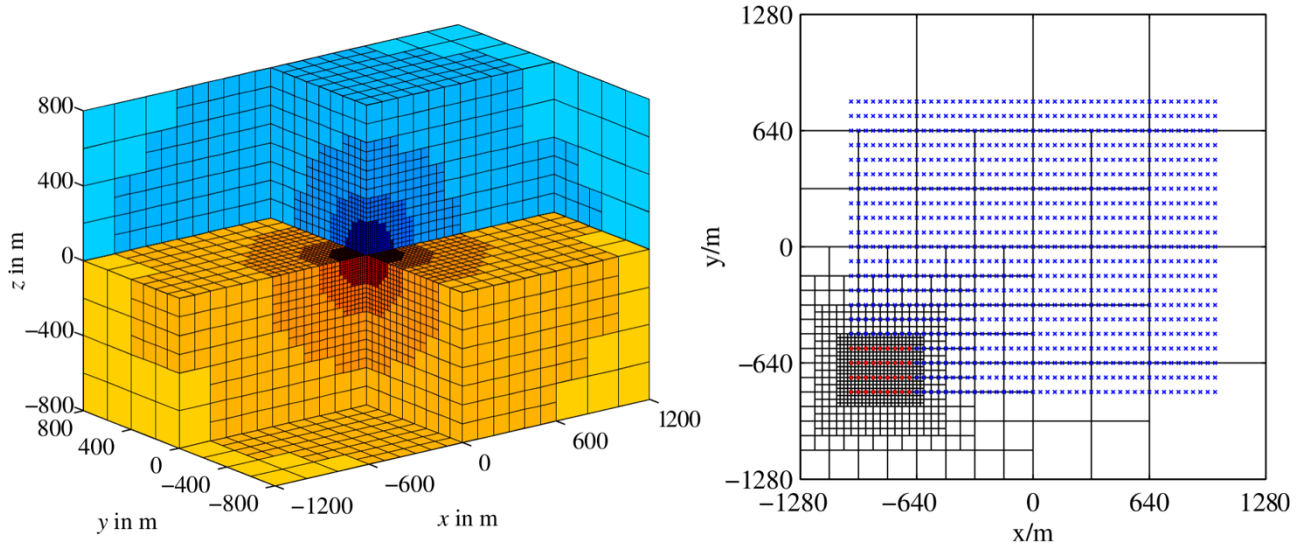


Figure 1 - Examples of locally refined octree meshes.

In our approach, the forward modelling mesh captures the entire domain. It is fine locally and coarse further away. Unlike the footprint approach, in our approach, the conductivity that is far away from the source/receiver position is averaged and is not ignored. In this way, we can treat large conductors that are far from the source but still influence the data. Using our methodology, we can compute the solutions for problems with thousands of sources in a reasonable time frame.

Our methodology uses a relatively small number of cells (roughly ten thousand) for each forward mesh which allows the use of direct solvers for the forward problem. Furthermore, our mesh generation process is quick and we can generate tens of thousands of meshes in a few minutes.

While we can model any anisotropic conductivity, the data rarely supports the inversion of a six-component tensor. To this end we model the anisotropic conductivity in each cell as

$$\Sigma = \begin{pmatrix} \sigma & 0 & 0 \\ 0 & \sigma & 0 \\ 0 & 0 & s\sigma \end{pmatrix}$$

Where σ is a conductivity and s is a horizontal to vertical scaling parameter. We start by inverting for σ assuming s is known and then we adjust s if we are unable to fit the data with a geologically reasonable model. When no a-priori information about anisotropy is given, we set $s = 1$ everywhere and obtain an isotropic conductivity. If the data or a-priori information justifies an anisotropic model, then in the second stage, we fix σ and invert for s , thus, obtaining an anisotropic model.

To first solve for σ , assume that data is collected for n_f frequencies and n_s sources and that the sources are discretized on n_s meshes. Let $A_{ij}(m)$ be the discrete linear system obtained by the discretization of Maxwell's equations with the i -th source and the j -th frequency with $m = \log(\sigma)$. We assume that the model m is discretised on an inversion mesh that is fine across the entire survey domain. To obtain the model for a particular forward problem, a much coarser interpolation is used. The main advantage of an OcTree mesh is that the forward meshes are nested within the inverse mesh, making the interpolation straight forward.

Finally, let P_{ij}^T be a matrix that projects the solution of the ij -problem to n_r receivers. Then the simulated data can be written in the form of a set of vectors

$$\mathbf{d}_{ij}(\mathbf{m}) = P_{ij}^T A_{ij}(\mathbf{m}, \mathbf{s})^{-1} \mathbf{q}_j \quad \text{for } i = 1, \dots, n_s, \quad j = 1, \dots, n_f$$

Let \mathbf{d}_{obs} be the observed data, that is, the data collected in the field. The goal of the first step of the ij -inversion is to estimate a log conductivity \mathbf{m} , given a fixed s such that $\mathbf{d}_{ij}(\mathbf{m}) \approx \mathbf{d}_{ij}^{obs}$ for $i = 1, \dots, n_s, j = 1, \dots, n_f$. Then, if required, we fix \mathbf{m} and estimate a scale factor s to produce a further improved data fit.

Let W_{ij} be the inverse covariance matrix for each data vector d_{ij} . Then, the misfit between the observed and predicted data can be written as

$$\mathfrak{J}_{mis}(\mathbf{m}, \mathbf{s}) = \frac{1}{n_s n_f} \sum_{ij} \|P_{ij}^T A_{ij}(\mathbf{m}, \mathbf{s})^{-1} \mathbf{q}_j - \mathbf{d}_{ij}\|_{W_{ij}}^2$$

where $\|\cdot\|_W$ is the W -weighted norm. Since the problem does not admit stable solutions, we use regularization in the form of smoothness and smallness. We define the discrete cell-centred gradient matrix G_c and use the regularization

$$\mathfrak{J}_{reg}(\mathbf{m}, \mathbf{s}) = \frac{1}{2} \|G_c(\mathbf{m} - \mathbf{m}_{ref})\|_V^2 + \frac{1}{2} \alpha_s \|\mathbf{m} - \mathbf{m}_{ref}\|_V^2 + \frac{1}{2} \|G_c(\mathbf{s} - \mathbf{s}_{ref})\|_V^2$$

where the matrix V contains weights that allow for different smoothing in different directions, \mathbf{m}_{ref} and \mathbf{s}_{ref} are model and scaling reference terms chosen to represent a-priori information. α_s is a smallness parameter. In typical inversions we set α_s to be very small compared to the weights in V .

The model is obtained by minimizing a linear combination of the misfit and the regularization

$$\min_{\mathbf{m}_L \leq \mathbf{m} \leq \mathbf{m}_H} \mathfrak{J}(\mathbf{m}, \mathbf{s}) = \mathfrak{J}_{mis}(\mathbf{m}, \mathbf{s}) + \alpha \mathfrak{J}_{reg}(\mathbf{m}, \mathbf{s})$$

where α is a regularization parameter and \mathbf{m}_L and \mathbf{m}_H are vectors of upper and lower bounds that are set based on geological a-priori information. We then use stochastic programming techniques, in particular the Stochastic Average Approximation (SAA), to approximate the sum over all the terms by a random subset. Then we use the Gauss-Newton method to solve each sub-problem as shown in Ruszczyński and Shapiro (2003).

SYNTHETIC EXAMPLE

In this section, we describe numerical experiments that demonstrate the capability of our code to deal with anisotropy in large scale problems. The survey consists of five 13km North-South lines spaced 1km apart as shown in Figure 2. Each line contains 15 transmitter locations where the transmitter is an 800m line source located at a depth of 10m below the air/water interface. For each transmitter, there are 15 receivers measuring in-line electric fields, evenly spaced 500m apart behind the transmitter. 13 linearly spaced frequencies are collected that range from 0.22 to 2.62 Hz. The true model consists of four layers with two resistive blocks buried at depth. The first two layers are isotropic with layer 1 being 300m of 0.3 Ωm sea-water and layer 2 containing 300m of 1.0 Ωm sediments. Layer 3 is 100m thick with a horizontal resistivity of 2.0 Ωm and a vertical conductivity of 4.0 Ωm while layer 4 extends to depth with a horizontal resistivity of 2.0 Ωm and a vertical resistivity of 1.5 Ωm . The isotropic resistive blocks are 50 Ωm and 100 Ωm , and buried from 1200m – 1300m and 1400m – 1600m respectively as shown in Figure 3. Figure 4 shows the scale factor between the true horizontal and vertical resistivity values.

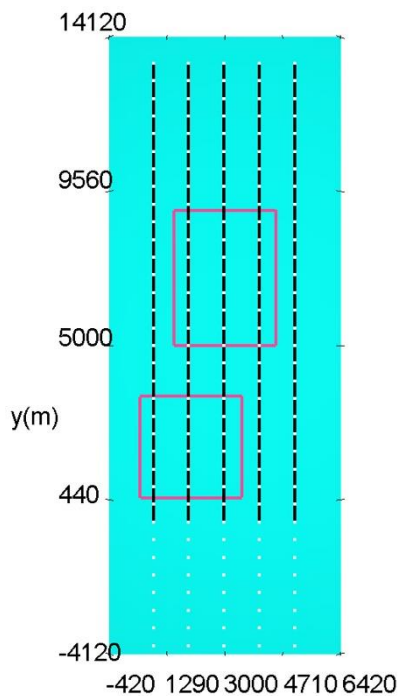


Figure 3 - Survey layout with transmitter lines in black, receiver locations in white.

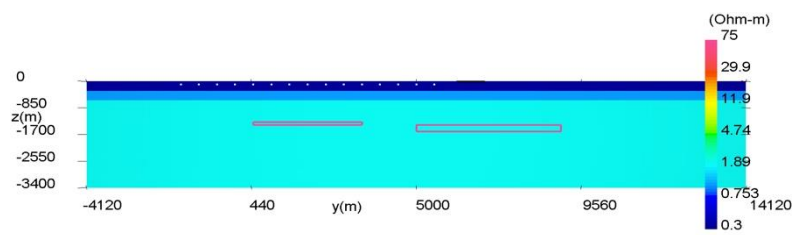


Figure 3 - North-South cross-section through the isotropic conductivity (σ) reference model. Receivers for one towed transmitter shown as white dots. Location of true resistive blocks shown in red.

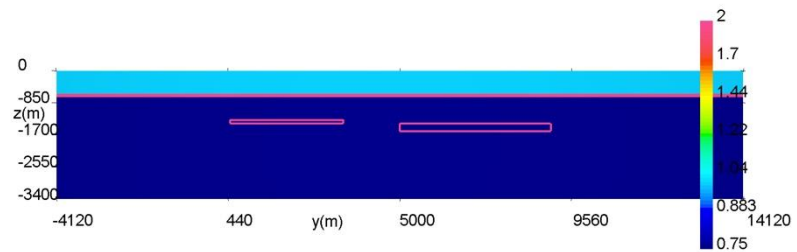


Figure 2 - North-South cross-section through the conductivity scale factor (s) reference model. Location of true resistive blocks shown in red.

For this simulated survey, we have 13,500 combinations of sources and frequencies. We use local OcTree meshes with a parallel system of 32 cores, each with a speed of 2.7GHz with every four cores sharing 32GB of RAM, allowing the simulation to be completed in less than 40 minutes. We first solve for σ on a mesh composed of 825,038 OcTree cells. The desired misfit of 2.5% from its initial value was obtained in 19 iterations with the whole inversion process taking about 17 hours to complete.

Figure 5 shows our isotropic inversion result using Figure 3 as a reference model. The two resistive blocks are identified but the depth of the deeper target is underestimated and the true resistivity values are too low. We also ran an anisotropic inversion where we fixed the horizontal resistivity and inverted for a scale factor model which produces the vertical resistivity. Figure 6 shows this scale factor model and Figure 7 shows the resulting vertical resistivity model. Figure 8 compares the isotropic and anisotropic results in plan view at 1300m depth. With the anisotropic code, there is a small improvement in the depth and true resistivity of the recovered target resistors compared to the isotropic result.

CONCLUSIONS

CSEM imaging techniques are now common but solving for anisotropic conductivity in 3D is still relatively new (Newman et al., 2010). In this work, we have implemented a two-stage anisotropic 3D CSEM inversion and applied the method to a realistic synthetic model.

In the first stage, we recover an isotropic conductivity model that does a reasonable job in depicting the true shape and conductivity of the target resistors. In the second stage, we fix the conductivity and solve for a scale factor that relates the vertical and horizontal conductivity in each mesh cell. The resulting vertical conductivity model is an improvement over the isotropic result in terms of both defining the true spatial extents and conductivity of the targets.

REFERENCES

- Haber, E. and Schwarzbach, C., 2014, Parallel inversion of large-scale airborne time-domain electromagnetic data with multiple OcTree meshes: *Inverse Problems*, 30(5), 1–28.
- Newman, G.A., Commer, M. and Carazzone, J.J., 2010, Imaging CSEM data in the presence of electrical anisotropy: *Geophysics*, 75(2), P51–P61.
- Ruszczynski, A. and Shapiro, A., 2003, *Stochastic programming*. Amsterdam: Elsevier.
- Schwarzbach, C., Haber, E. and Columbia, B., 2011, Finite element based inversion for electromagnetic problems using stochastic optimization: 81st Annual International Meeting, SEG, Expanded Abstracts, 30, 567–572.

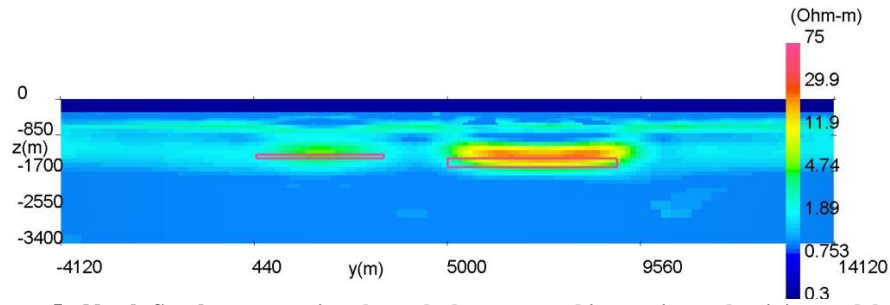


Figure 5 - North-South cross-section through the recovered isotropic conductivity model (σ). Location of true resistive blocks shown in red

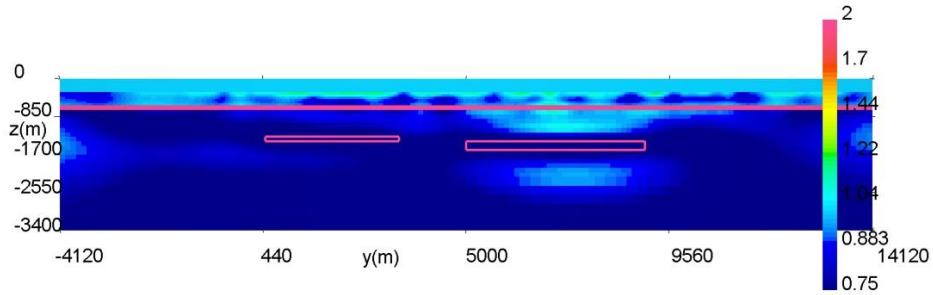


Figure 6 - North-South cross-section through the recovered conductivity scale factor (s) model. Location of true resistive blocks shown in red.

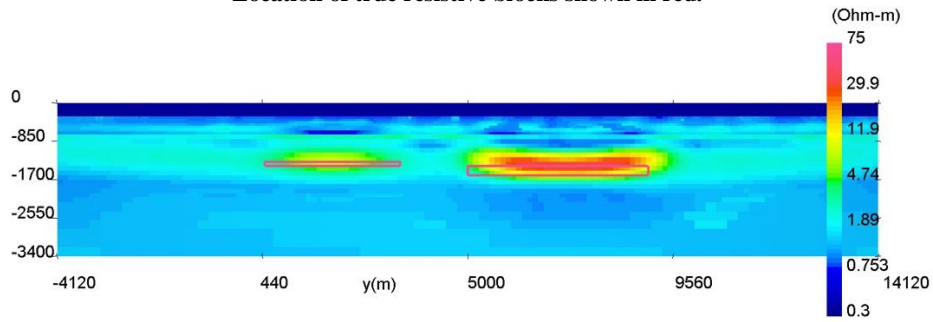


Figure 7 - North-South cross-section through the recovered vertical conductivity model (σ_v). Location of true resistive blocks shown in red. Note the slight improved depth of the recovery resistors

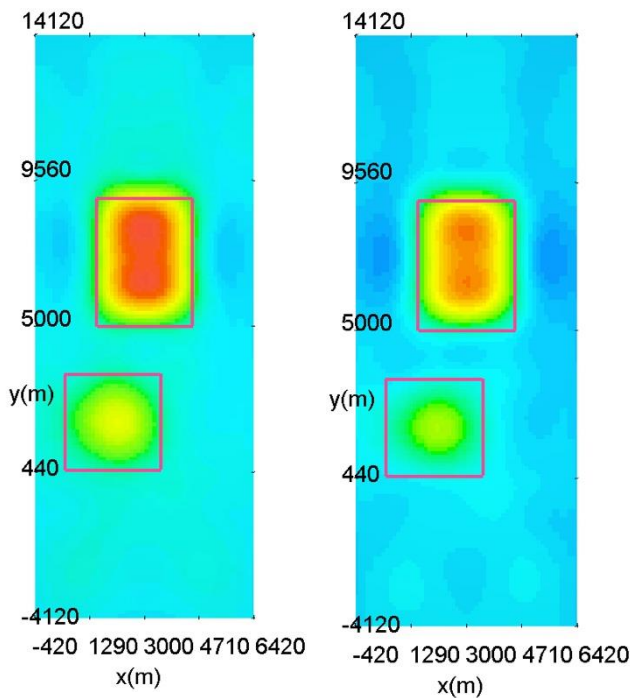


Figure 8 - Plan slice at 1300m depth through the recovered isotropic conductivity model (σ , left pane) and the recovered vertical conductivity model (σ_v , right pane). Location of true resistive blocks shown in red